

# Novel DCE-MRI Technique: Application to Breast Cancer

D. Artemov<sup>1</sup>, W. Zhu<sup>1</sup>, and Y. Kato<sup>1</sup>

<sup>1</sup>Radiology, Johns Hopkins University, Baltimore, MD, United States

**Introduction:** Increased microvessel density and increased permeability of the vascular bed are important biomarkers of malignancy and are detected in aggressive breast cancer. These parameters can be assessed by dynamic contrast-enhanced MRI (DCE-MRI) that has been used to determine the tumor grade, extent of disease, and treatment response (1, 2). In breast cancer DCE-MRI studies have reported high sensitivity, but lower specificity and until now a universal strategy for analysis of breast DCE-MRI has not been formulated. One approach is an empirical, model-free evaluation of contrast uptake by enhancement curves pattern, “three time point” parametric images, or semi-quantitative techniques that use parameters such as time of maximum enhancement and maximum enhancement time ratio derived from DCE-MRI data (3, 4). The analytical approach to DCE-MRI analysis requires fitting of experimental data to a physiological model such as two-compartment pharmacokinetic model to derive the fractional volume of the extracellular extravascular space ( $v_e$ ), the transfer constant characterizing reflux of GdDTPA from the  $v_e$  into the plasma compartment ( $k_{ep}$ ), and the transfer constant characterizing extravasation of GdDTPA from the plasma ( $K^{trans}$ ) (5). This model is applicable only if several important assumptions are met including (i) fast exchange of water between all compartments including cellular water; (ii) precise determination of the arterial input function (AIF) for  $C_p(t)$ , (iii) no artifacts from inflowing fresh blood, (iv) unambiguous determination of tissue contrast concentrations from the signal enhancement. For instance, if water exchange is not fast parameters  $K^{trans}$  and  $v_e$  can be underestimated by up to 300% (6). In part due to these problems there is no currently accepted way to present analytical data measured by DCE-MRI. One approach is to use a simulated arterial input curve and report  $K^{trans}$  as absolute units (or percent enhancement) per minute or derive relative  $K^{trans}$ ,  $k_{ep}$  and  $v_e$  parameters (7, 8). In many reports the measured values of  $K^{trans}$  and  $v_e$  are larger than 1.0 that is physically impossible.

**Methods:** MRI experiments that use saturation recovery with a short recovery delay such as gradient echo with short repetition time and 90-degree flip angle are inherently insensitive to water exchange kinetics (9-11). Here we present a 3D sequence developed using this idea that is designed and optimized for GdDTPA enhanced DCE-MRI (Fig. 1A). Important features of the method that facilitate quantitative analysis are (i) 90-degree flip angle and short recovery time (20ms) provide insensitivity to water exchange kinetics; (ii) non-selective saturation of the whole volume with hard pulses removes artifacts from inflowing fresh blood; (iii) each phase encoding step starts with the complete saturation, therefore the sequence does not need to be executed in a steady-state mode; (iv) because of the previous condition, a slice with well-delineated blood vessels can be imaged more frequently in comparison to the complete 3D or multi-slice 2D map for precise determination of AIF with high temporal resolution. Example of kinetic analysis performed for a large tumor with enhancing rim is shown in Fig. 1B and demonstrates excellent fitting of the experimental data using the standard two-compartment model.

Experiments to compare vascular parameters of two tumor models were performed on a Bruker horizontal bore 9.4T animal MR scanner using SCID mice inoculated with MCF-7 and MDA-MB-231 cells in opposite flanks. GdDTPA was administered i.v. into the tail vein (0.5 mmoles/kg as 0.1ml bolus over 10 sec), 3D MR acquisition was performed for 24x18x10 mm field of view with a matrix size of 128x64x16. The interleaved 2D single-slice imaging with the whole-volume hard pulse saturation recovery and a slice thickness of 1.25 mm was performed for 128x64 matrix. Acquisition times were ~40 sec and ~5 sec per frame for 3D and 2D acquisition, respectively.

**Results and Discussion:** Typical images of a mouse with inoculated tumors and a plot of tissue concentrations of the contrast agent as a function of time are presented in Fig. 2. Tissue concentrations were fitted to the equation

$$C_t(t) = K^{trans} \int_0^t C_p(\tau) e^{-k_{ep}(t-\tau)} d\tau$$

using a non-linear POWELL minimization algorithm programmed in IDL environment. Signal intensity generated by the sequence is proportional to the GdDTPA tissue concentration and is to a larger extent independent on the water exchange kinetics as well as on T2 and T2\* in a particular voxel. This is especially important for measuring of AIF, since high GdDTPA plasma concentrations often

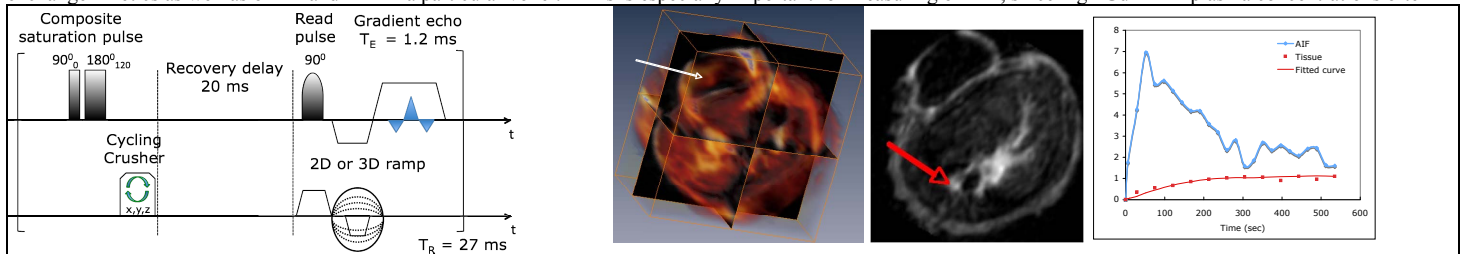


**Figure 1A.** Diagram of the pulse sequence with non-selective saturation, short recovery time, and 2D or 3D acquisition with 90-degree RF pulse.

**Figure 1B.** 3D reconstruction of the DCE-MRI data set. White arrow points to the enhancing tumor region that was analyzed by the model. Red arrow shows the position of the blood vessel used for AIF measurements in both 3D and interleaved 2D images (the AIF sampling rate was doubled in comparison to tissue concentrations).

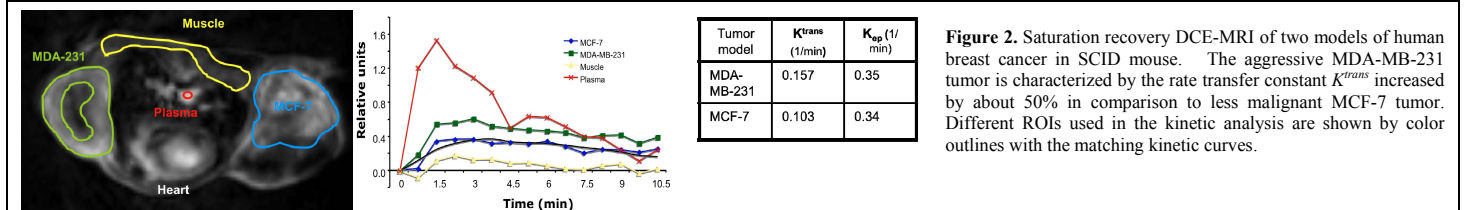


**Figure 2.** Saturation recovery DCE-MRI of two models of human breast cancer in SCID mouse. The aggressive MDA-MB-231 tumor is characterized by the rate transfer constant  $K^{trans}$  increased by about 50% in comparison to less malignant MCF-7 tumor. Different ROIs used in the kinetic analysis are shown by color outlines with the matching kinetic curves.

lead to nonlinear effects in MR measurements. The important feature of the method is that the fast 2D acquisition can be arbitrarily interleaved with 3D imaging because precise timing of the consecutive acquisitions is not important for the method (due to the complete saturation of magnetization at each step). If segmented 3D acquisition is used, the AIF can be sampled in an optimal way i.e. with high temporal resolution at the beginning of the experiment and gradually reducing towards the end of the study. In our experiments a simple [2D,3D,2D,3D,...] interleaved scheme was used that provided a two-fold increase in the temporal resolution of the AIF sampling in comparison to the tissue contrast agent measurements as shown in Figs. 1 and 2.

**Acknowledgements:** This work was supported by NIH P50 CA103175. We thank Dr. Zaver Bhujwala for valuable discussions and support and Mr. Gary Cromwell for technical assistance.

**References:** 1. Knopp MV et al. J Magn Reson Imaging 1999; 10: 260-6. 2. Jacobs MA et al. Technol Cancer Res Treat 2004; 3: 543-50. 3. Degani H et al. Nat Med 1997; 3: 780-2. 4. Turnbull LW. NMR Biomed 2009; 22: 28-39. 5. Tofts PS et al. J Magn Reson Imaging 1999; 10: 223-32. 6. Yankeelov TE et al. Magn Reson Imaging 2007; 25: 1-13. 7. Manton DJ et al. Br J Cancer 2006; 94: 427-35. 8. Radjenovic A et al. Br J Radiol 2008; 81: 120-8. 9. Kim YR et al. Magn Reson Med 2002; 47: 1110-20. 10. Schwickert HC et al. Magn Reson Med 1995; 34: 845-52. 11. Zhu W et al. ISMRM 18th Scientific Meeting and Exhibition; 2010; 4804.